9-1-2020

NGC 474 as viewed with KCWI: Diagnosing a shell galaxy

Adebusola B. Alabi
University of California, Santa Cruz

Anna Ferre-Mateu
Universitat de Barcelona

Duncan A. Forbes
Swinburne University of Technology

Aaron J. Romanowsky
San Jose State University, aaron.romanowsky@sjsu.edu

Jean P. Brodie
University of California, Santa Cruz

Recommended Citation

Adebusola B. Alabi, Anna Ferre-Mateu, Duncan A. Forbes, Aaron J. Romanowsky, and Jean P. Brodie. "NGC 474 as viewed with KCWI: Diagnosing a shell galaxy" *Monthly Notices of the Royal Astronomical Society* (2020): 626-631. https://doi.org/10.1093/mnras/staa1992

Monthly Notices of the ROYAL ASTRONOMICAL SOCIETY

MNRAS **497,** 626–631 (2020) doi:10.1093/mnras/staa1992
Advance Access publication 2020 July 9

NGC 474 as viewed with KCWI: diagnosing a shell galaxy

Adebusola B. Alabi [1,2]★ Anna Ferré-Mateu [3] Duncan A. Forbes,[2]
Aaron J. Romanowsky [1,4] and Jean P. Brodie[1,2]

[1]*University of California Observatories, 1156 High Street, Santa Cruz, CA 95064, USA*
[2]*Centre for Astrophysics and Supercomputing, Swinburne University, Hawthorn, VIC 3122, Australia*
[3]*Institut de Ciencies del Cosmos (ICCUB), Universitat de Barcelona (IEEC-UB), E-02028 Barcelona, Spain*
[4]*Department of Physics and Astronomy, One Washington Square, San José State University, San Jose, CA 95192, USA*

Accepted 2020 July 3. Received 2020 July 2; in original form 2020 May 23

ABSTRACT

We present new spectra obtained using Keck/KCWI and perform kinematics and stellar population analyses of the shell galaxy NGC 474, from both the galaxy centre and a region from the outer shell. We show that both regions have similarly extended star formation histories although with different stellar population properties. The central region of NGC 474 is dominated by intermediate-aged stars (8.3 ± 0.3 Gyr) with subsolar metallicity ($[Z/H] = -0.24 \pm 0.07$ dex) while the observed shell region, which hosts a substantial population of younger stars, has a mean luminosity-weighted age of 4.0 ± 0.5 Gyr with solar metallicities ($[Z/H] = -0.03 \pm 0.09$ dex). Our results are consistent with a scenario in which NGC 474 experienced a major to intermediate merger with a $\log(M_*/M_\odot) \sim 10$ mass satellite galaxy at least ∼2 Gyr ago which produced its shell system. This work shows that the direct spectroscopic study of low-surface brightness stellar features, such as shells, is now feasible and opens up a new window to understanding galaxy formation and evolution.

Key words: galaxy: evolution – galaxy: formation – galaxies: individual (NGC 474).

1 INTRODUCTION

NGC 474 is perhaps best known for its spectacular system of stellar shells (Malin & Carter 1983; Forbes 1999; Turnbull, Bridges & Carter 1999; Duc et al. 2015). Shells, alongside similar faint stellar tidal features, e.g. streams, loops, plumes, rings, etc. are telltale signatures of the hierarchical assembly of present-day galaxies and are believed to have formed during galaxy mergers or close galaxy interactions (Schweizer 1980; Quinn 1984; Dupraz & Combes 1986; Hernquist & Quinn 1988; Thomson & Wright 1990; Thomson 1991; González-García & Balcells 2005; Kado-Fong et al. 2018; Pop et al. 2018; Karademir et al. 2019).

NGC 474, classified as a type II shell system (Prieur 1988), is the dominant S0 galaxy (Pierfederici & Rampazzo 2004) in the Arp 227 group. It has a projected spatial separation of 5.4 arcmin (∼47 kpc) from its nearest neighbour (the spiral galaxy NGC 470), with both galaxies having identical systemic velocities. While it is clear that the gas-poor NGC 474 is interacting with its gas-rich neighbour (Schiminovich et al. 1997; Cullen, Alexander & Clemens 2006; Rampazzo et al. 2006; Mancillas, Combes & Duc 2019a), the debate about the origin of the observed shell system and its evolutionary link with the ongoing interaction is still open (Schombert & Wallin 1987; Forbes 1999). Furthermore, assuming the observed shells have a merger origin, then the nature of the merger event (major/minor) as well as the nature of the disrupted satellite(s) are both unclear.

The central region of NGC 474 has been well studied spectroscopically: with long-slit spectroscopy (e.g. Hau, Balcells & Carter 1996; Caldwell, Rose & Concannon 2003; Denicoló et al. 2005) and with IFU (integral field unit) spectroscopy as part of the SAURON project (Bacon et al. 2001) and the ATLAS^{3D} survey (Cappellari et al. 2011). These IFU studies reported an average luminosity-weighted age and metallicity of 7.4 Gyr and −0.1 dex within 1 effective radius (R_e), respectively, and an α-element enhancement, [α/Fe], of 0.17 dex in Kuntschner et al. (2010) and McDermid et al. (2015). NGC 474 is one of the very few fast-rotating galaxies from the ATLAS^{3D} survey with significant misalignment between its photometric and kinematic axis (Emsellem et al. 2007; Krajnović et al. 2011). A similar result was presented earlier from the long-slit spectroscopic study of Hau et al. (1996). More generally, spectroscopic studies dedicated to shell galaxies have hitherto focused exclusively on the central galaxy regions (e.g. Longhetti et al. 1998; Hau, Carter & Balcells 1999; Carlsten, Hau & Zenteno 2017), while the stellar shells (usually located in the galaxy outskirts) have not been probed due to their low surface brightness.

In this paper, we show that direct starlight spectroscopy of stellar shells and streams is now feasible with more sensitive integral field spectrographs such as the new Keck Cosmic Web Imager (KCWI; Morrissey et al. 2018) at Keck. We extend the exploration of the central regions in shell galaxies and build on previous work where discrete tracers such as globular clusters were used to probe shells and streams (Romanowsky et al. 2012; Foster et al. 2014; Lim et al. 2017; Alabi et al. 2020). We present results from our KCWI IFU spectroscopic observation of NGC 474, covering both the galaxy centre and a region of the outer shell with mean V-band surface brightness 22.0 and 25.4 mag arcsec^{-2}, respectively. Throughout this work, we adopt a distance of 29.5 Mpc to NGC 474 (Tully et al. 2013),

★ E-mail: aalabi@ucsc.edu

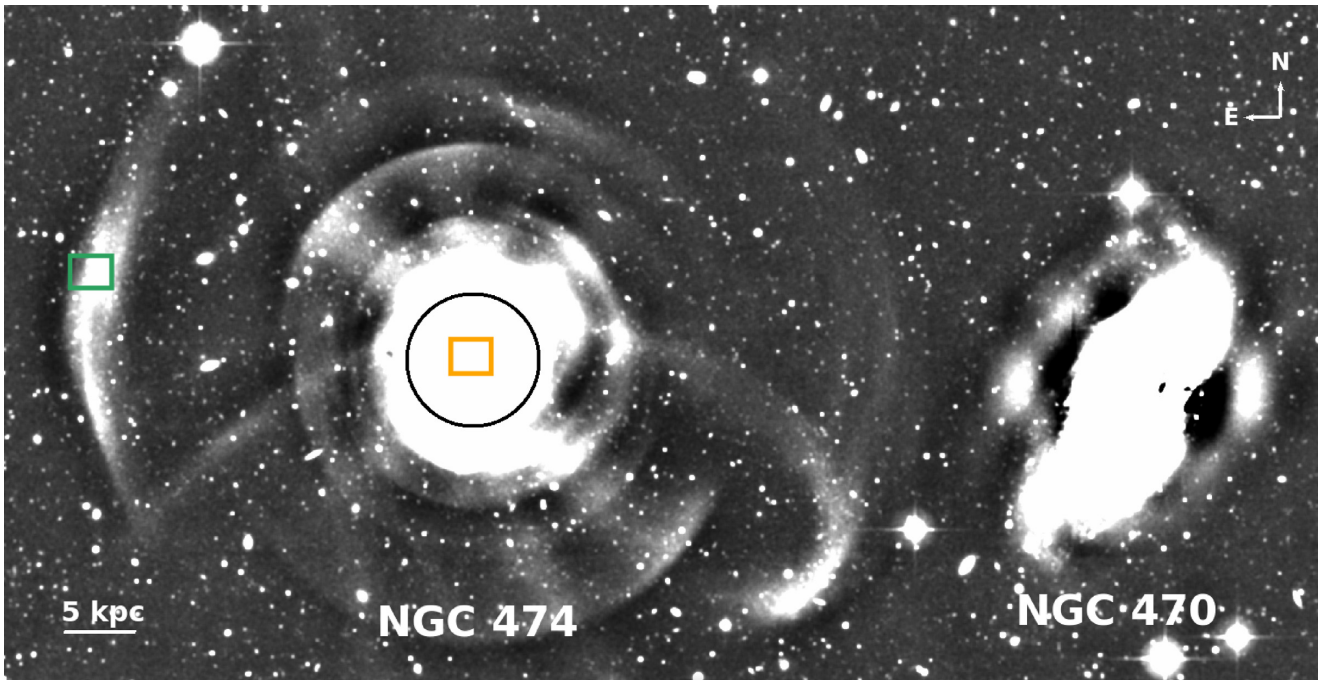

Figure 1. Combined image of NGC 474 from archival CFHT/MegaCam *g*, *r*, and *i* images. The image shows the spectacular system of stellar shells and plumes in NGC 474 and covers 11 arcmin × 5.5 arcmin which corresponds to 94 × 47 kpc at the distance of NGC 474. The spiral galaxy NGC 470 is at a projected distance of ∼47 kpc away from NGC 474. The orange and green rectangles, each equivalent to 2.4 × 2.9 kpc, show the central and shell regions we have observed with Keck/KCWI, respectively. For reference, the black circle is the 1 effective radius isophote and the white horizontal line has a length of 5 kpc. The observed shell region is at a physical distance of ∼30 kpc away from the centre of the galaxy.

$R_e = 33$ arcsec or 4.7 kpc (Cappellari et al. 2011), and a logarithmic stellar mass of $\log(M_*/M_\odot) \sim 10.6$ from 3.6 μm *Spitzer* imaging (Sheth et al. 2010).

2 OBSERVATIONS AND DATA

We obtained spectroscopic data from the central and shell regions of NGC 474 with the KCWI during the nights of 2017 September 19 and October 18. We used the BM grating centred at $\lambda_c = 4800$ Å and the medium image slicer to obtain spectral data with nominal resolution $R \sim 4000$. This configuration spans the spectral region 4360–5230 Å and has a 16.5 arcsec × 20.4 arcsec field-of-view. We therefore obtained data with spectral resolution FWHM = 1.2 Å or $\sigma_{\rm instr} \sim 32\,{\rm km\,s^{-1}}$ at λ_c. We observed the galaxy centre for 600 s and a region of the prominent eastern shell for a total of 4800 s, with both regions shown in Fig. 1. Our observed shell region was chosen to have maximum brightness along the shell but free of compact, point sources such as globular clusters or foreground stars. We also observed a dedicated blank field for accurate sky subtraction.

Standard data reduction was performed with the publicly available KCWI pipeline – KDERP[1] – although we used a custom-made PCA code to perform sky subtraction (see Gannon et al. 2020 for details). This is because extra attention has to be paid to sky subtraction especially in the case of spectral data from low surface brightness features such as the stellar shells which are typically ≥100 × fainter than the night sky. We collapsed by median-stacking all the useable spaxels within the combined, sky-subtracted fields into single 1D spectra, and obtained final galaxy centre and shell spectra with signal-to-noise (S/N) ratios of ∼43 and ∼15 per Å, respectively. We show these spectra in Fig. 2.

[1] https://github.com/Keck-DataReductionPipelines/KcwiDRP

3 CENTRAL AND SHELL STELLAR KINEMATICS

We measured the line-of-sight velocities and stellar velocity dispersions at the galaxy centre and from the outer shell region with the upgraded version of the `pPXF` (Cappellari & Emsellem 2004; Cappellari 2017) code. For our kinematics analysis, we employed the empirical ELODIE stellar library (Prugniel & Soubiran 2001) which has a spectral resolution FWHM = 0.51 Å (or $\sigma \sim 13\,{\rm km\,s^{-1}}$) at λ_c. This allowed us to probe down to (and possibly below) intrinsic velocity dispersions comparable to the instrumental resolution, which may well be the case in the outer shell regions. We obtained a radial velocity of $2324 \pm 6\,{\rm km\,s^{-1}}$ and a velocity dispersion of $134 \pm 6\,{\rm km\,s^{-1}}$ for the central pointing, consistent with measurements in the literature. Note that this velocity dispersion, measured within an $R_e/3$ effective aperture, is aperture corrected following the prescription of Jorgensen, Franx & Kjaergaard (1995). For the outer shell region, we measured a radial velocity of $2325 \pm 8\,{\rm km\,s^{-1}}$ and a velocity dispersion of $18 \pm 9\,{\rm km\,s^{-1}}$.

4 STELLAR AGE, METALLICITY, AND STAR FORMATION HISTORY OF NGC 474

As shown in Fig. 2, the spectra from both the galaxy central and shell regions include age- and metallicity-sensitive absorption features such as Hβ, Fe5015, and Mg*b* (although the latter is on the edge of the spectra). The difference between the outer shell and the central part of the galaxy is already noticeable from their spectra. The outer

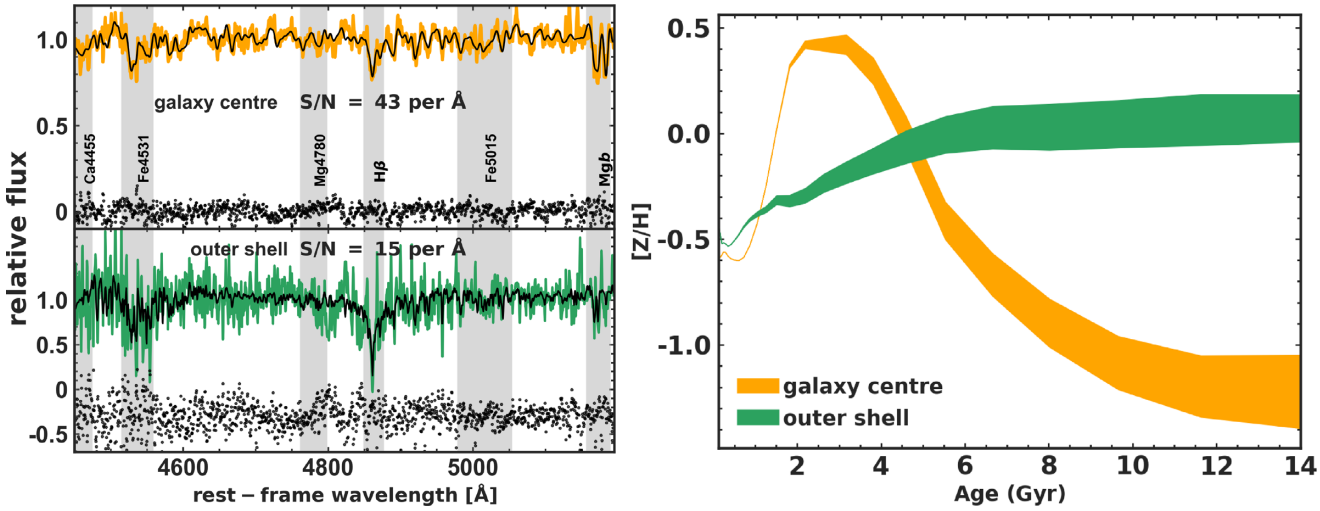

Figure 2. Left-hand panel: Sky subtracted, median normalized Keck/KCWI spectra from the galaxy central region (*upper panel*) and the outer shell region (*lower panel*) of NGC 474, with best-fitting STECKMAP models shown as black spectra in both panels. Residuals from the best-fit are shown in the lower part of each panel (shifted by −0.3 in the lower panel for display purpose only), and the prominent absorption features within the rest-frame spectral range have been identified and labelled. Note the relative strength of the H β feature in the *lower panel* compared to the *upper panel*, hinting at the presence of a substantial, younger stellar population in the outer shell region. Right-hand panel: Age–metallicity relations from the galaxy centre and the outer shell region. The width of each band corresponds to the stellar mass fractions at different ages. The bands highlight the different chemical evolutionary histories of the galaxy centre and the outer shell region.

shell spectrum shows a factor of ∼3 enhancement in the equivalent width of the H β feature compared to the galaxy centre spectrum. As H β is a strong age indicator, this already suggests the presence of a substantial population of younger stars in the shell region.

We perform full spectral fitting with the non-parametric regularized STECKMAP software (Ocvirk et al. 2006a,b) in order to obtain the mean age and metallicity estimates and the star formation histories from both regions. For this exercise, we use the medium resolution ($R = 10\,000$) PÉGASE-HR library of stellar population spectra (Prugniel & Soubiran 2001; Le Borgne et al. 2004) computed with a Salpeter initial mass function at scaled-solar abundances. We model our spectra as a linear combination of these template spectra with ages and metallicities spanning 0.1 to 14 Gyr and −2.0 to 0.2 dex, respectively. The best-fitting models and residuals are shown in Fig. 2. We adopt regularization parameters $\mu_x = 100$ and $\mu_Z = 10$ to smooth the stellar age–metallicity relation shown in Fig. 2, and note that the mean stellar population parameters are robust against changes in these values. As suggested by several authors, (e.g. Sánchez-Blázquez et al. 2011; Ruiz-Lara et al. 2015), we fit the stellar population properties separately from the stellar kinematics obtained in the previous section due to possible degeneracies between stellar velocity dispersion and metallicity. We summarize our results in Table 1 and provide the mean mass- and luminosity-weighted stellar ages and total metallicities ([Z/H]).

As suggested earlier from the strong H β feature, the luminosity-weighted age of the outer shell region is 4.0 ± 0.5 Gyr – reflecting the increased contribution from young stars to the outer shell spectrum – while the galaxy centre has an older mean luminosity-weighted age of 7.2 ± 0.4 Gyr. In contrast, the mass-weighted stellar ages from both galaxy regions are similar, differing by only ∼1 Gyr. The mean luminosity-weighted ages give a sense of when the last star formation episode occurred whereas the mean mass-weighted age estimates are directly linked to the epoch when the bulk of the stellar mass was formed.

The galaxy centre has a mean mass-weighted [Z/H] value of -0.24 ± 0.07 dex, while the shell region is slightly more metal-rich (by 0.21 ± 0.11 dex, almost at the 2σ level) with a mean mass-weighted [Z/H] value of -0.03 ± 0.09 dex. This relatively metal-rich nature of the outer shell region agrees with the metallicity signatures reported in the shell galaxy sample from the Illustris cosmological simulation (Pop et al. 2017). We note that the mean luminosity-weighted [Z/H] from the shell region is similar to the measurement from the galaxy centre. This is because luminosity-weighted [Z/H] reflects the chemical composition of the underlying old stellar population (Serra & Trager 2007). The central ages and metallicities compare well with previous results from the literature (Kuntschner et al. 2010; McDermid et al. 2015) and also agree with the [Z/H]–σ scaling relation from Spolaor et al. (2010).

Table 1. Summary of results from kinematics and stellar population analyses from both central and shell regions. Parameters with mass and lum subscripts are mass- and luminosity-weighted, respectively.

Parameter	Centre	Shell
$V_{\rm los}$ (km s^{-1})	2324 ± 6	2325 ± 8
σ (km s^{-1})	134 ± 6	18 ± 9
Age $_{\rm mass}$ (Gyr)	8.3 ± 0.3	7.1 ± 0.5
[Z/H] $_{\rm mass}$ (dex)	−0.24 ± 0.07	−0.03 ± 0.09
Age $_{\rm lum}$ (Gyr)	7.2 ± 0.4	4.0 ± 0.5
[Z/H] $_{\rm lum}$ (dex)	−0.14 ± 0.08	−0.16 ± 0.06

Fig. 3 shows the star formation histories from the galaxy centre and the outer shell region. As expected from fast-rotating, low-mass galaxies in low-density environment (Kauffmann et al. 2004; McDermid et al. 2015; Bernardi et al. 2019), we obtain evidence of extended star formation from both regions of NGC 474. The galaxy centre formed half of its stellar mass within the first ∼3 Gyr while it took a more extended period of ∼5 Gyr for the outer shell to build up half its stellar mass. Although both regions have extended star formation histories, Fig. 3 shows that the shell region experienced

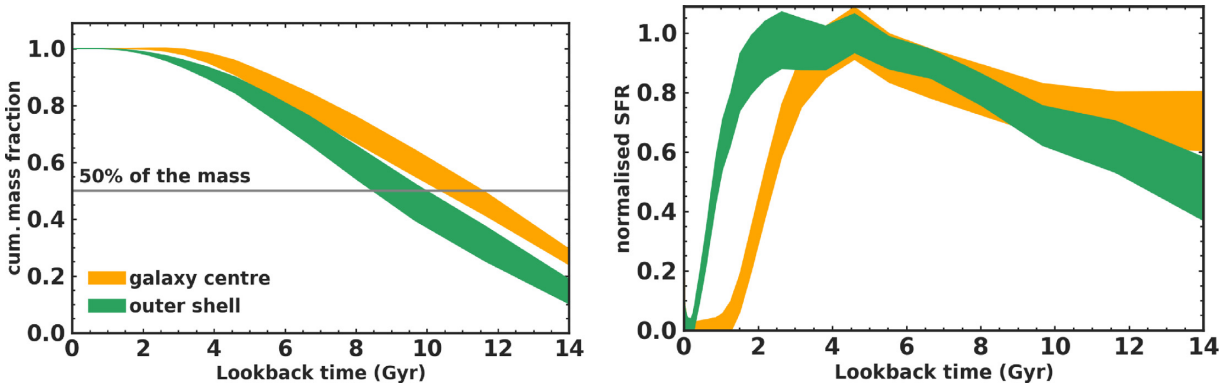

Figure 3. Star formation history from the galaxy centre (orange colour) and the outer shell region (green colour). Both regions of NGC 474 experienced extended star formation but peak star formation at different epochs. The *left-hand panel* shows cumulative mass fraction as a function of lookback time. The orange and green bands show the standard errors around the mean values obtained from Monte Carlo simulations. The horizontal line shows how long it takes to build up 50 per cent of the total stellar mass. The *right-hand panel* shows the normalized star formation rate. The outer shell region experienced a more recent peak of star formation rate (in the last ∼2 Gyr) than the central region of the galaxy.

a more recent star formation peak within the last ∼2 Gyr. Since our stellar population modelling was done assuming solar abundances, and the lack of a red continuum around the Mg*b* feature makes a direct line-index evaluation of [α/Fe] impossible, we use equation (3) from McDermid et al. (2015) and the time taken to build up half-mass to estimate [α/Fe] of ∼0.19 dex and ∼0.15 dex in the galaxy centre and shell region, respectively. This [α/Fe] estimate for the galaxy centre is consistent with the results from Kuntschner et al. (2010) and McDermid et al. (2015).

5 DISCUSSION

Our kinematics analysis shows that the radial velocity from the shell region is identical to that of the galaxy centre. Analytical models have shown that the sharp stellar density maxima which define shells are only seen at the apocentres along the orbital path of the infalling galaxies, where the mean shell velocity should be comparable to that of the host galaxy (Merrifield & Kuijken 1998; Sanderson & Helmi 2013). Our result confirms this observationally and can be used in the future to discriminate bona fide shells from other tidal stellar features when spatially resolved 2D velocity maps become available. From these models, it is not obvious what the velocity dispersion in the shell regions should be relative to the galaxy centre. However, one expects stellar shells to be dynamically cold substructures with low velocity dispersions (Sanderson, Mohayaee & Silk 2012). The velocity dispersion we have measured in the outer shell region is lower (at the ∼2σ level) compared to what is measured in $\log(M_*/\mathrm{M}_\odot) \sim 10.6$ galaxies at similar projected radii (Napolitano et al. 2009; Foster et al. 2016).

Our stellar population analysis shows that NGC 474 has an extended star formation history. This is consistent with expectations for intermediate mass galaxies in low-density environments (Kauffmann et al. 2004). The galaxy centre is dominated (in luminosity and mass) by subsolar metallicity ([*Z*/H] = −0.24 ± 0.07 dex and −0.14 ± 0.08 dex, respectively) intermediate-age stars (7–8 Gyr). On the other hand, the stellar population properties of the outer shell region are more complicated. Its age (mass-weighted) and metallicity (luminosity-weighted) are similar to the galaxy centre, but it also hosts a substantial population of younger stars (mean luminosity-weighted age of 4.0 ± 0.5 Gyr) with solar metallicities (mean mass-weighted [*Z*/H] = −0.03 ± 0.09 dex). The outer shell region is slightly more metal-rich compared to the galaxy centre by 0.21 ± 0.11 dex, significant almost at the 2σ level. These differences are also captured in the stellar age–metallicity relation of each galaxy region (right-hand panel in Fig. 2). The stellar population properties of the stars in the outer shell region therefore suggest an ex-situ origin and an evolutionary path different from the galaxy centre. This also agrees with the conclusions from cosmological simulations (Pop et al. 2018; Karademir et al. 2019; Mancillas et al. 2019a). However, this does not completely resolve the issue of the origin of the shells – are the shells made from stellar materials accreted from the nearby NGC 470 or are they relics of a disrupted satellite galaxy?

NGC 470 is known to be undergoing an intense nuclear starburst (Friedli et al. 1996) and in a study of the Arp 227 group, Rampazzo et al. (2006) found H I tidal tails extending from NGC 470 towards the east of NGC 474, in the direction of our shell region (see their fig. 4). Based on the H I flux in the tidal tails they argued that the gas accretion is in its early stages. Using the maximum rotation velocity of the H I gas in NGC 470 (240 km s^{-1}), we estimate a time-scale of ∼0.3 Gyr for accreted materials to be deposited in the shell region (at a projected distance of 77 kpc). This time-scale is inconsistent with the mean luminosity-weighted age we have measured for the stars in the outer shell, and thus rules out the ongoing interaction with NGC 470 as the sole origin of the observed shell system. Therefore, a disrupted satellite seems to be the more plausible scenario for the formation of the shell system in NGC 474. While we have assumed the simplest merger scenario that involves a single disrupted galaxy, we note that there is observational evidence from the different colours of the various shells in NGC 474 that suggests a multiple merger origin, with further support from cosmological simulations (Pop et al. 2018). Addressing the question of the multiple merger origin of the stellar shells in NGC 474 is however outside the scope of this study.

The stellar population properties of the stellar shell can shed more light on the origin and nature of the disrupted galaxy. Our analysis above shows that the outer stellar shell is young and metal-rich. Using the galaxy mass–metallicity relation from Gallazzi et al. (2005), the outer shell's mass-weighted metallicity of [*Z*/H] = −0.03 dex suggests that the disrupted galaxy had a stellar mass of $\log(M_*/\mathrm{M}_\odot) \geq 9.6$. This estimate agrees well with the conclusion made by Lim et al. (2017) that the disrupted galaxy is overmassive for a dwarf galaxy but still sub-L^*. Kim et al. (2012), using *Spitzer* imaging, already reported that the shells in NGC 474 are ∼6−10 percent as luminous as the underlying galaxy light (see their table 4). If we assume that a single merger event produced the

observed shell system and use the finding from the *N*-body simulation of Hernquist & Spergel (1992) that shells typically contain ∼25 per cent of the total stars in the disrupted galaxy, then the disrupted galaxy most likely had a stellar mass of $\log(M_*/M_\odot) \sim 10$. These results show that the shells of NGC 474 most likely originated from an intermediate to major merger event with mass ratio of 1 : 9 to 1 : 3. Bearing in mind that shells are usually visibile for 3–4 Gyr after they first appear (Thomson 1991; Pop et al. 2018; Mancillas et al. 2019b) and that mergers are likely to induce star formation (e.g. Barnes 2004), it is possible that the enhancement in the star formation rate from the outer shell region at ∼2 Gyr is directly connected to the merger event that produced it.

6 CONCLUSION

We have obtained the kinematics and stellar population properties from the galaxy centre and an outer shell region of NGC 474 using new spectral data obtained from Keck with KCWI. We argue that the spectacular stellar shells seen around NGC 474 have an ex-situ origin in agreement with expectations from cosmological simulations and were most likely formed in a major or intermediate (mass ratios 1 : 3 – 1 : 9) merger event with a metal-rich progenitor ∼2 Gyr ago. Since then, NGC 474 has been accreting cold gas from the outskirts of its gas-rich, spiral galaxy neighbour (NGC 470), which is currently undergoing a starburst. This first, direct spectroscopic observation of the low surface brightness, outer shell region of NGC 474 with Keck/KCWI shows that invaluable insights about the nature of nearby stellar shells in nearby galaxies can now be efficiently obtained on 10 m telescopes with deep spectroscopy.

ACKNOWLEDGEMENTS

We thank the anonymous referee for the thoughtful reading of the manuscript and for the valuable feedback. We thank I. Martin-Navarro and A Wasserman for help with the observations. AFM acknowledges financial support from LCF/BQ/LI18/11630007. AJR was supported by National Science Foundation grant AST-1616710 and as a Research Corporation for Science Advancement Cottrell Scholar. DAF thanks the ARC for financial support via DP160101608. ABA and JPB gratefully acknowledge support from National Science foundation grants AST- 1518294 and AST-1616598.

The data presented herein were obtained at the W. M. Keck Observatory, which is operated as a scientific partnership among the California Institute of Technology, the University of California, and the National Aeronautics and Space Administration. The Observatory was made possible by the generous financial support of the W. M. Keck Foundation. The authors wish to recognize and acknowledge the very significant cultural role and reverence that the summit of Maunakea has always had within the indigenous Hawaiian community. We are most fortunate to have the opportunity to conduct our research from this mountain.

DATA AVAILABILITY

The observational data underlying this article are available online and can be accesed on the Keck Observatory Archive (KOA), which is operated by the W. M. Keck Observatory and the NASA Exoplanet Science Institute (NExScI), under contract with the National Aeronautics and Space Administration.

REFERENCES

Alabi A. B., Forbes D. A., Romanowsky A. J., Brodie J. P., 2020, MNRAS, 491, 5693
Bacon R. et al., 2001, MNRAS, 326, 23
Barnes J. E., 2004, MNRAS, 350, 798
Bernardi M., Domínguez Sánchez H., Brownstein J. R., Drory N., Sheth R. K., 2019, MNRAS, 489, 5633
Caldwell N., Rose J. A., Concannon K. D., 2003, AJ, 125, 2891
Cappellari M., 2017, MNRAS, 466, 798
Cappellari M., Emsellem E., 2004, PASP, 116, 138
Cappellari M. et al., 2011, MNRAS, 413, 813
Carlsten S. G., Hau G. K. T., Zenteno A., 2017, MNRAS, 472, 2889
Cullen H., Alexander P., Clemens M., 2006, MNRAS, 366, 49
Denicoló G., Terlevich R., Terlevich E., Forbes D. A., Terlevich A., Carrasco L., 2005, MNRAS, 356, 1440
Duc P.-A. et al., 2015, MNRAS, 446, 120
Dupraz C., Combes F., 1986, A&A, 166, 53
Emsellem E. et al., 2007, MNRAS, 379, 401
Forbes D. A., 1999, in Impey C., ed., International Symposium on Astrophysics Research and Science Education. p. 228
Foster C. et al., 2014, MNRAS, 442, 3544
Foster C. et al., 2016, MNRAS, 457, 147
Friedli D., Wozniak H., Rieke M., Martinet L., Bratschi P., 1996, A&AS, 118, 461
Gallazzi A., Charlot S., Brinchmann J., White S. D. M., Tremonti C. A., 2005, MNRAS, 362, 41
Gannon J. S., Forbes D. A., Romanowsky A. J., Ferré-Mateu A., Couch W. J., Brodie J. P., 2020, MNRAS, 495, 3
González-García A. C., Balcells M., 2005, MNRAS, 357, 753
Hau G. K. T., Balcells M., Carter D., 1996, in Bender R., Davies R. L., eds, Proc. IAU Symp. 171, New Light on Galaxy Evolution. Kluwer Academic Publishers, Berlin, Germany, p. 388
Hau G. K. T., Carter D., Balcells M., 1999, MNRAS, 306, 437
Hernquist L., Quinn P. J., 1988, ApJ, 331, 682
Hernquist L., Spergel D. N., 1992, ApJ, 399, L117
Jorgensen I., Franx M., Kjaergaard P., 1995, MNRAS, 276, 1341
Kado-Fong E. et al., 2018, ApJ, 866, 103
Karademir G. S., Remus R.-S., Burkert A., Dolag K., Hoffmann T. L., Moster B. P., Steinwandel U. P., Zhang J., 2019, MNRAS, 487, 318
Kauffmann G., White S. D. M., Heckman T. M., Mnard B., Brinchmann J., Charlot S., Tremonti C., Brinkmann J., 2004, MNRAS, 353, 713
Kim T. et al., 2012, ApJ, 753, 43
Krajnović D. et al., 2011, MNRAS, 414, 2923
Kuntschner H. et al., 2010, MNRAS, 408, 97
Le Borgne D., Rocca-Volmerange B., Prugniel P., Lançon A., Fioc M., Soubiran C., 2004, A&A, 425, 881
Lim S. et al., 2017, ApJ, 835, 123
Longhetti M., Rampazzo R., Bressan A., Chiosi C., 1998, A&AS, 130, 251
Malin D. F., Carter D., 1983, ApJ, 274, 534
Mancillas B., Combes F., Duc P. A., 2019a, A&A, 630, A112
Mancillas B., Duc P.-A., Combes F., Bournaud F., Emsellem E., Martig M., Michel-Dansac L., 2019b, A&A, 632, A122
McDermid R. M. et al., 2015, MNRAS, 448, 3484
Merrifield M. R., Kuijken K., 1998, MNRAS, 297, 1292
Morrissey P. et al., 2018, ApJ, 864, 93
Napolitano N. R. et al., 2009, MNRAS, 393, 329
Ocvirk P., Pichon C., Lançon A., Thiébaut E., 2006a, MNRAS, 365, 46
Ocvirk P., Pichon C., Lançon A., Thiébaut E., 2006b, MNRAS, 365, 74
Pierfederici F., Rampazzo R., 2004, Astron. Nachr., 325, 359
Pop A.-R., Pillepich A., Amorisco N., Hernquist L., 2017, Galaxies, 5, 34
Pop A.-R., Pillepich A., Amorisco N. C., Hernquist L., 2018, MNRAS, 480, 1715
Prieur J. L., 1988, ApJ, 326, 596
Prugniel P., Soubiran C., 2001, A&A, 369, 1048
Quinn P. J., 1984, ApJ, 279, 596
Rampazzo R. et al., 2006, MNRAS, 368, 851

Romanowsky A. J., Strader J., Brodie J. P., Mihos J. C., Spitler L. R., Forbes D. A., Foster C., Arnold J. A., 2012, ApJ, 748, 29
Ruiz-Lara T. et al., 2015, A&A, 583, A60
Sánchez-Blázquez P., Ocvirk P., Gibson B. K., Pérez I., Peletier R. F., 2011, MNRAS, 415, 709
Sanderson R. E., Helmi A., 2013, MNRAS, 435, 378
Sanderson R. E., Mohayaee R., Silk J., 2012, MNRAS, 420, 2445
Schiminovich D., van Gorkom J., van der Hulst T., Oosterloo T., Wilkinson A., 1997, Imaging and Kinematics of Neutral Hydrogen in and around 'Shell Galaxies'. p. 362
Schombert J. M., Wallin J. F., 1987, AJ, 94, 300
Schweizer F., 1980, ApJ, 237, 303
Serra P., Trager S. C., 2007, MNRAS, 374, 769
Sheth K. et al., 2010, PASP, 122, 1397
Spolaor M., Kobayashi C., Forbes D. A., Couch W. J., Hau G. K. T., 2010, MNRAS, 408, 272
Thomson R. C., 1991, MNRAS, 253, 256
Thomson R. C., Wright A. E., 1990, MNRAS, 247, 122
Tully R. B. et al., 2013, AJ, 146, 86
Turnbull A. J., Bridges T. J., Carter D., 1999, MNRAS, 307, 967

This paper has been typeset from a TEX/LATEX file prepared by the author.